VAPOR–SOLID GROWTH OF InP AND Ga_2O_3 BASED COMPOSITE NANOWIRES

D. Jishiashvili[a]*, Z. Shiolashvili[a], N. Makhatadze[a], A. Jishiashvili[a], V. Gobronidze[a] and D. Sukhanov[a]

Presented at 3rd International Conference "Nanotechnologies", October 20 – 24, 2014, Tbilisi, Georgia (Nano – 2014)

Keywords: core-shell nanowire, indium phosphide, gallium(III) oxide.

InP/Ga_2O_3 core-shell nanowires were grown on Si substrate at 400 ºC in the hydrazine (N_2H_4) vapor diluted with 3 mol. % H_2O. The crystalline InP and solid Ga served as source materials for the growth of nanowires. According to TEM and EDX data the nanowires consisted of InP core with wurtzite-type structure and an amorphous Ga_2O_3 shell. The minimum diameter of NWs was 14 nm, while the maximum lengths reached several micrometers. The twinned planes appeared in WZ InP core at increased nanowire diameters. Based on the obtained results and possible chemical reactions, the following mechanism was proposed for the growth of core-shell nanowires: pyrolytic decomposition of hydrazine caused the appearance of intermediate NH_2, NH and H species in the vapor. At elevated temperatures the crystalline InP source was also dissociated to In and phosphorus precursors. At source temperatures close to 600 ºC, due to the interaction of In and Ga sources with water molecules and hydrazine decomposition products the volatile Ga_2O and In_2O were formed. These molecules reached the Si substrate which was heated to 400 ºC. The final chemical reaction involved Ga_2O_3, In_2O_3 and phosphorus precursors. As a result of a spontaneous reaction the Ga_2O_3 and InP phases were produced and segregated. The InP crystallized as a core while Ga_2O_3 created the amorphous shell, because the growth temperature was insufficient for its crystallization.

* Corresponding Author
E-Mail: d_jishiashvili@gtu.ge
[a] V. Chavcanidze Institute of Cybernetics, Georgian Technical University, 0186, Euli Str. 5, Tbilisi, Georgia

Introduction

The core-shell nanostructures are considered as the promising building blocks for the future advanced nanodevices.[1-3] The unique properties of core-shell nanostructures arise not only from quantum confinement and surface dominated features, but also due to the processes that take place in the shell material and core–shell interface. The band gap of core semiconductor and its emission profile can be preciously tuned by selecting the proper composition and thickness of a shell material, without altering the size of core nanoparticle.[4-7] The latest demonstration of the use of biofunctionalized InP/ZnS core-shell nanocrystals raised interest in the development of future nanoprobes for biomedical applications, that may replace the highly toxic cadmium-based nanostructure with less toxic InP based biomarkers.[5,8,9]

Together with zero dimensional (0D) core-shell nanocrystals the 1D core-shell nanostructures (nanowires, nanotubes, nanorods, nanobelts etc.) also attracted a great interest and show promise for different applications. Ultrasensitive toxic-gas sensors were fabricated recently using various core–shell nanowires (NWs).[10-13] This type of 1D nanostructures were also successfully used for light emitting diodes,[14-16] for the fabrication of solid quantum bits[17] and nanowire lasers,[18] for the effective solar energy conversion,[19] etc.

1D nanostructures with InP cores are considered as promising materials not only due to the unique electronic and optical properties of indium phosphide, but also for their potential wide range of applications in different fields beginning from telecommunications and ending with biological imaging. Indium phosphide offers a "green" alternative to the traditional cadmium-based biomarkers, but suffers from extreme susceptibility to oxidation. Coating InP cores with more stable shell materials significantly improves the resistance to oxidation and photostability [5, 20], thus increasing the interest of scientists in the development of new InP based core-shell nanostructures.

The purpose of this work was to develop the one-step process for the growth of InP based core–shell nanowires.

Experimental

The nanowires were grown in the tubular vertical quartz reactor which was first evacuated and then filled with hydrazine (N_2H_4) vapor to its saturated pressure of ~ 10 Torr. The piece of a flat crystalline InP covered with coarsely ground metallic Ga served as a source for producing volatile species. The source was placed at the bottom of the reactor and annealed in the presence of hydrazine vapor which was containing 3 mol. % water molecules. The weight ratio of InP and Ga was 2.5 at a total mass of 0.50 – 0.55 g. In the presence of hydrazine decomposition products the volatile compounds were formed at the surfaces of Ga and InP sources, which after sublimation caused the growth of ID nanomaterials on the Si substrate placed at 2 cm above the source.

The Si substrate temperature (growth temperature) was in the range of 400 – 430 °C, which corresponded to the source temperature of 600 – 635 °C. The nanowire growth time of was 45 – 60 min. The details of the growth technology are presented elsewhere.[21]

The morphology and structure of NWs were studied using FEI Quanta FEG 600 scanning electron microscope (SEM). Transmission electron microscopy (TEM) images were recorded on a Philips CM12 operated at 100 keV with a W cathode and a FEI Tecnai F30 (FEG) equipped with an energy dispersive X-ray (EDX) and a high-angle annular dark-field (HAADF) detector The Gibbs free energies for the chemical reactions were evaluated using the computer software HSC Chemistry–6 and chemical database stored in this program.

Results and discussion

The whole growth process was based on the transportation of constituent atoms from the source material (solid InP and Ga) located in the hot zone of the reactor (T_{max} = 635 °C) to the Si substrate placed at 2 cm distance just above the source (cold zone, T_{max} = 430 °C). The vertical quartz reactor operated at a static pressure (10 Torr) of N_2H_4 + 3 mol. % H_2O vapor and was isolated from the vacuum system during the growth of nanowires. In the absence of carrier gases only vaporized and volatile molecules could reach the substrate surface. The convectional flow, which appeared due to the temperature difference between source and substrate also promoted the transportation of volatile species.

The pyrolytic decomposition of hydrazine in the presence of 3 mol. % H_2O leads to a variety of highly reactive fragments. The detailed study of ammonia and hydrazine decomposition at elevated temperatures was presented in Ref.[22,23] Decomposition of hydrazine can usually be performed by two methods: catalytic decomposition (for example on semiconductor or metal source surfaces, or heated quartz reactor walls) and thermal decomposition.[24,25] Following active intermediate species were formed during the decomposition: NH_2, NH, N, H, until the final stabile products (N_2, H_2) were produced. Besides, the dissociative adsorption of hydrazine may take place with the formation of two NH_2 radical species on the source surface. The strong nitriding ability and activity of hydrazine decomposition products was confirmed in our previous experiments on the growth of single crystalline Ge_3N_4 1D nanowires at 500 ºC using volatile GeO molecules as germanium precursors.[26] In this growth process the temperature was by 350 ºC lower in comparison with the synthesis of Ge_3N_4 nanowires using the same GeO source molecules and ammonia vapor.[27,28] We assume, that such a dramatic reduction of nitriding temperature in hydrazine vapor can be explained only by the high concentration of active NH_2 and/or NH species, together with possible presence of atomic nitrogen. It should be noted that the single crystalline, pure germanium nitride NWs and micrometer sized crystalline blocks were obtained in hydrazine vapor in spite of the presence of oxidizing water molecules in it (3 mol. % H_2O).[26] Besides, the chain like pure germanium nanostructures were formed on the substrate and no traces of GeO or GeO_2 were found in the condensed material.[21] This proves a high reducing ability of hydrazine vapor. On the nanoscale range the high activity of hydrazine was confirmed in numerous works on the reduction of graphene layer at room temperature from its oxide using hydrazine (see for example Ref.[29]).

The thermal decomposition of InP source in the reactor served for producing gaseous phosphorus ambient and In precursors. As it was found in Ref.[30, 31] in the presence of hydrogen the InP dissociation temperature can be significantly decreased. For example, the energy of activation of dissociation reaction

$$InP_{(solid)} = In_{(solid)} + ½P_{2(gas)}$$

is reduced from 154.5 kJ mol^{-1} down to 38.9 kJ mol^{-1}, and InP dissociates at 297 ºC in the presence of atomic hydrogen with the concentration of 10^{15} cm^{-3}. The total amount of N_2H_4 molecules is $4.8 \cdot 10^{17}$ cm^{-3} in our reactor with the volume of 1.5 L at 10 Torr. This amount of hydrazine is sufficient to produce molecular or atomic hydrogen with concentration that will be close to concentrations described in Ref.[30,31] Accordingly, the decrease of InP dissociation temperature in our experiments has a sound physical bases and seems quite realistic. Besides, as it was found in Ref.,[30, 31] the phosphine (PH_3) appeared in the gaseous phase together with P_4, and the pressure of diphosphorus (P_2) increased up to 10^{-5} Torr. As a result of dissociation the In islands with diameters of several micrometers appeared at the surface of InP source. These In droplets together with metallic Ga, which was placed on the InP surface, served in our experiment as sources for the growth of NWs.

The transportation of Ga and In to the Si substrate surface needs the formation of volatile molecules. As it will be shown later, both elements were found in NWs grown on Si substrate located at 2 cm above the sources. The possible chemical reactions that lead to the formation of volatile suboxides will be suggested below to explain how these elements reached the Si substrate. The only volatile species that could perform this task are Ga and In suboxides (Ga_2O and In_2O). The water molecules diluted in hydrazine and some residual oxygen in the reactor are considered to be the only sources for producing oxides. Analyzing the Gibbs free energy of formation it was concluded that the first step in the formation of suboxides was the oxidation of metals to Ga_2O_3 and In_2O_3, with their subsequent reduction to suboxides using the hydrazine decomposition products (NH_2, NH, H). All these reactions have negative Gibbs free energy. The examples of chemical reactions are presented for the Ga source, but the similar tendency was observed also for the interaction of In source with the same reagents. The equations below have the tentative nature as they were calculated for 600 ºC and atmospheric pressure while the initial pressure in our experiments was 10 Torr. 600 ºC was selected as the reaction temperature because it corresponded to the temperature of our source. The first step is the oxidation of In and Ga:

$$2Ga + 3H_2O(g) = Ga_2O_3 + 3H_2(g) \quad \Delta G = –208 \text{ kJ mol}^{-1}$$

$$2Ga + 1.5O_2(g) = Ga_2O_3 \quad \Delta G = –807 \text{ kJ mol}^{-1}$$

Next step is the formation of volatile suboxides:

$$Ga_2O_3 + 2NH_2(g) = 2H_2O(g) + Ga_2O(g) + N_2(g)$$
$$\Delta G = -194 \text{ kJ mol}^{-1}$$

$$Ga_2O_3 + 4H(g) = Ga_2O(g) + 2H_2O(g)$$
$$\Delta G = -442 \text{ kJ mol}^{-1}$$

$$Ga_2O_3 + 4NH(g) = 2H_2O(g) + Ga_2O(g) + 2N_2(g)$$
$$\Delta G = -1188 \text{ kJ mol}^{-1}$$

The sign of ΔG determines only whether or not a chemical reaction will occur. The negative signs of ΔG in the equations listed above indicate that these reactions may take place spontaneously. However, the real amount of synthesized material depends on the reaction kinetics, i.e. on the rates of chemical processes. As a result of these reactions the volatile Ga_2O and In_2O molecules were produced. They reached the Si substrate heated up to 400 ºC and formed nanowires after reacting with ambient gases (P_2, P_4, PH_3, H_2O and O_2).

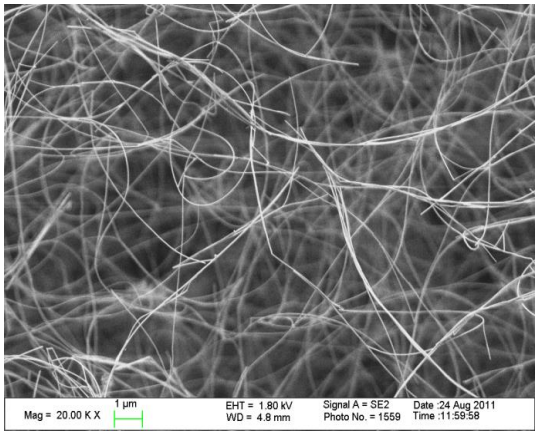

Figure 1. SEM image of nanowires grown on the Si substrate.

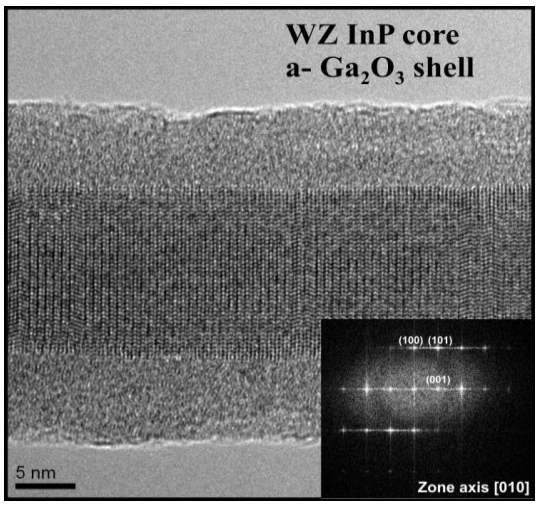

Figure 2. High resolution TEM image of InP/Ga_2O_3 nanowire with the average diameter of 28 nm (core – 14.9 nm). The Fast Fourier Transform (inset) confirms the WZ-type structure of the core.

Figure 1 presents SEM image of nanowires grown on the Si substrate. Some of them are quite long reaching tens of micrometers. The detailed structure of nanowires was studied using TEM and the results are presented in Figure 2 and Figure 3. As can be seen, the nanowires consist of crystalline core and the amorphous shell. The analysis of shell composition will be considered later. It should be noted that all nanowires presented on the surface of Si substrate have the heterogeneous core–shell structure and no nanowire were found with a homogeneous composition. Besides, no catalyst tips were observed, indicating that the growth proceeded through the vapor–solid mechanism with crystalline InP as a nucleation site.

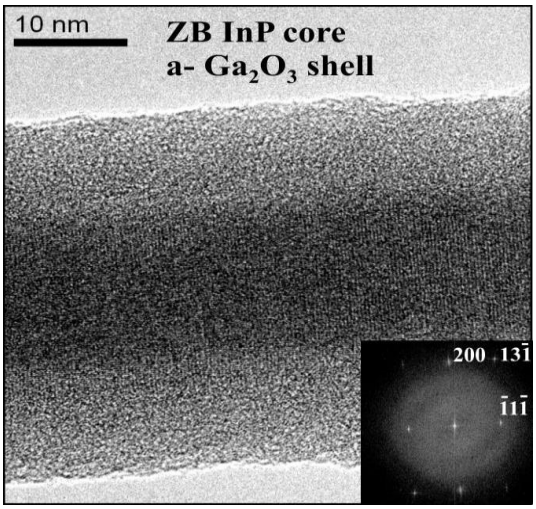

Figure 3. TEM image of ZB InP/amorphous Ga_2O_3 shell nanowire with the average diameter of 37.3 nm (core – 15.7 nm). Inset shows the ZB structure of nanowire that grows along [111] direction.

Analyzing the TEM results it was established that most nanowires have the cores of crystalline InP with wurtzite (WZ) structure. This is indicated in the Fast Fourier Transform in the inset of Figure 2, which shows a clear wurtzite pattern. In contrast to bulk non-nitride III–V materials which are usually zincblende (ZB) type, NWs predominantly crystallize as wurtzite type phases. Several different theoretical explanations for this behavior have been proposed. Recent calculations suggest that the WZ phase is energetically favorable for small NW radii.[32] Small radius results in a larger relative contribution of the nanowire sidewall surfaces to the total free energy. The surface dangling bonds at the nanowire lateral facets also have a significant influence on the formation of WZ structure. In Ref.[33] it was shown that the formation of wurtzite phase leads to an approximate 25 % reduction in the sidewall surface energy, and hence is thermodynamically favorable. A few core/shell nanowires were found, which preserved the ZB structure in spite of their small diameters (Figure 3). The reason for this phenomenon is not yet explained.

As it was mentioned earlier the WZ structured InP has significantly lower dangling bonds at the side walls as compared with ZB InP. This would cause the formation of less strained transition layer between WZ InP and the amorphous, unordered gallium oxide, because a low density of interface bonds will not alter significantly the side wall alignment.

Analyzing the side walls of InP in Figure 2 and Figure 3 one can detect the sharp interface between WZ InP and amorphous Ga_2O_3 in contrast to the rough and blurred ZB InP/Ga_2O_3 interface with possibly higher stresses.

Twin planes are the dominating stacking foults for III–V nanowires, which preferentially grow in the [111]B direction. Randomly positioned twin planes form naturally as a consequence of the relatively low twin-plane energy (about 10 mJ m^{-2} for InP).[34] This energy barrier is easily overcome at the typical growth temperatures and relatively high supersturation used in general. For nanowires larger than ~ 40 nm in diameter, the twinning between wurtzite and zinc-blende phases becomes quite frequent.[35] The same was observed in our nanowires. TEM images reflected the gradual increase of twin density for NWs with larger diameters, as it is demonstrated in Figure 4. The high density of rotational twins is clearly seen in TEM image of NW with the diameter of 74 nm (Figure 4). It is interesting to note that some rare twins can be clearly detected also in the high resolution TEM image in Figure 2.

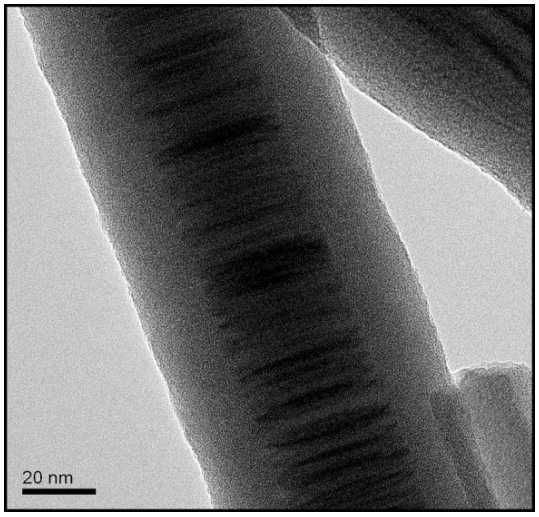

Figure 4. TEM image of InP/Ga_2O_3 core–shell nanowire with rotational twins. The diameter of nanowire was 74 nm.

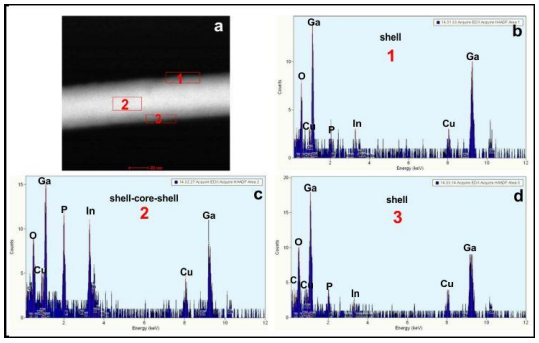

Figure 5. HAADF STEM image of the nanowire (a) and EDX spectra of rectangular regions marked in (a) (b – d).

The composition of a shell was studied by the EDX method. Figure 5 shows the HAADF STEM image of NW and three EDX spectra. Two of them were obtained from the rectangular shell regions marked by 1 and 3 (Figure 5b and 5d). Figure 5c reflects the composition of two shells and a core, because the focused excitation electron beam was transmitting the NW, initiating the simultaneous emission of X-rays from core and two shells located above and behind the core. As can be seen, In an P peaks increase in the core, while shells contain mainly Ga and oxygen. Comparison of these results with EDX spectrum of pure Ga_2O_3 powder confirmed that the shell material can be attributed to the gallium(III) oxide. The peak of Cu in the spectra comes from the copper TEM grid.

When considering the possible mechanisms of the core-shell nanowire formation it should be emphasized that the gallium oxide shell has an amorphous structure, as it was produced at 400 ºC. This temperature is insufficient for the crystallization because, to our knowledge, 610 ºC is the minimum temperature for the growth of crystalline Ga_2O_3 (β modification) using Ga_2O precursors.[36] According to TEM images in Figures 2 – 4, the thickness of Ga_2O_3 shell is quite uniform along the nanowire length and it depends on the nanowire core diameter. It increases with the increase of a core diameter, indicating that the core and shell were produced simultaneously, through the unified chemical reaction.

From the other hand, if we assume that Ga_2O_3 was formed separately, then it would appear on the substrate in the form of the deposited amorphous layer, because the formation of amorphous nanowires in the absence of templates (tubular pores or template nanowires) is impossible. According to the assumption made above, the Ga_2O_3 shell was deposited on the side walls of InP nanowire core during the whole growth time. This would lead to the formation of tapered core–shell NWs. However the tapering was not observed in SEM and TEM images of grown nanowires, confirming that the assumption concerning the separate deposition of Ga_2O_3 shell was wrong and the shells were formed simultaneously with InP through the spontaneous chemical reaction.

The spontaneous growth is a process driven by the reduction of Gibbs free energy realized by chemical reaction or phase transformation.[37] Taking into account the existing precursors the possible chemical reactions that may lead to the spontaneous formation of InP-Ga_2O_3 core-shell nanowires were analyzed. We suggest following reactions for the formation of core–shell NWs at T = 400 ºC:

$$Ga_2O(g) + 2In_2O(g) + 4PH_3(g) = Ga_2O_3 + 4InP + 6H_2(g)$$

$$\Delta G = -799 \text{ kJ mol}^{-1}$$

$$Ga_2O(g) + 2In_2O(g) + 2P_2(g) = Ga_2O_3 + 4InP$$

$$\Delta G = -798 \text{ kJ mol}^{-1}$$

$$Ga_2O(g) + 2In_2O(g) + P_4(g) = Ga_2O_3 + 4InP$$

$$\Delta G = -672 \text{ kJ mol}^{-1}$$

These reactions have sufficiently high negative values of Gibbs free energy to form the core-shell nanowires with the composition that were observed in our experiments. It should be emphasized once again that these reactions have the tentative nature because the standard state thermodynamic data were used for their calculation. However, we consider that these equations can truly convey the main tendencies of NW formation observed in this work.

Taking into account that the whole Si substrate was covered with a thick "mat" of nanowires, like those depicted in Figure 1, it can be concluded that considered chemical equations have significant reaction rates.

Conclusions

The core-shell nanowires were grown on Si substrate at 400 ºC in the hydrazine vapor diluted with 3 mol. % H_2O. The crystalline InP and solid Ga served as source materials for the growth of nanowires. According to TEM and EDX data the nanowires consisted of wurtzite InP core with an amorphous Ga_2O_3 shell. The twinned planes appeared in WZ InP core at increased nanowire diameters. Based on the obtained results and possible chemical reactions, the following mechanism was proposed for the growth of core-shell nanowires: pyrolytic decomposition of hydrazine caused the appearance of active intermediate NH_2, NH and H species in the vapor. At elevated temperatures the crystalline InP source was also dissociated to In and phosphorus precursors. At source temperatures close to 600 ºC, due to the interaction of In and Ga sources with water molecules and hydrazine decomposition products the volatile Ga_2O and In_2O were formed. These molecules reached the Si substrate which was heated to 400 ºC. The final chemical reaction involved Ga_2O_3, In_2O_3 and phosphorus precursors. As a result of a spontaneous reaction the Ga_2O_3 and InP phases were produced and segregated. The InP crystallized as a core while Ga_2O_3 created the amorphous shell, because the growth temperature was insufficient for its crystallization.

Acknowledgments

The authors are thankful to Professor Dr. Greta R. Patzke and Dr. Roman Kontic (University of Zurich, Institute of Inorganic Chemistry, Zurich, Switzerland) for permanent help in experimental work and discussions.

References

[1]Qi, W., Luo, L., Qian, H.-Sh., Ouyang, G., Nanda, K. K., Obare, Sh. O., (Eds.). *Core–Shell Nanostructures: Modeling, Fabrication, Properties, and Applications. J. Nanomater.*, **2012** – Special Issue.

[2]Reiss, P., Protiere, M., Li, L., *Small*, **2009**, *5*, 154.

[3]Choi. H.-J., In: *Nano Science and Technology* (Ed. G.-C. Yi), *Berlin – Heidelberg: Springer–Verlag,* **2012**.

[4]Lei, D., Shen, Y. T., Feng, Y., Feng. W., *Sci. China: Technol. Sci*., **2012**, *55*, 903.

[5]Kim, S., Shim, W., Seo, H., Bae, J. H., Sung. J., Choi, S. H., Moon, W. K., Lee, G., Lee, B., Kim, S.-W., *Chem. Commun.*, **2009**, *10*, 1267.

[6]Lu, M.-Y., Zhou, X., Chiu, C.-Y., Crawford, S., Gradečak, S., *ACS Appl. Mater. Interfaces*, **2014**, *6*, 882.

[7]Marcu, A., Enculescu, I., Vizireanu, S., Birjega, R., Porosnicu, C., *Dig. J. Nanomater. Biost.*, **2013,** *8*, 597.

[8]Dennis, A. M., Piryatinski, A., Mangum, B. D., Park, Y.-Sh., Htoon, H., Hollingsworth, J. A., *243rd American Chemical Society National Meeting &Exposition. Chemistry of Life. Section: Basic Research in Colloids, Surfactants and Nanomaterials.* **2012**, San Diego, Pub. # 97.

[9]Mushonga, P., Onani, M. O., M. Madiehe, A., Meyer. M., *J. Nanomater.*, **2012,** *2012*, 11 pp.

[10]Li, X., Li, X., Chen, N., Li, X., Zhang, J., Yu, J., Wang, J., Tang, Zh., *J. Nanomater.*, **2014,** *2014*, 7 pp.

[11]Le, D. T. T., Trung, D. D., Chinh, N. D., Binh, B. T. T., Hong, H. S., Duy, N. V., Hoa, N. D., Hieu, N. V., *Curr. Appl. Phys.*, **2013,** *13*, 1637.

[12]Jang, Y.-G., Kim, W.-S., Kim, D.-H., Hong, S.-H., *J. Mater. Res.*, **2011**, *26*, 2322.

[13]Chen, C., Lin, Sh.-Sh., Lin, T.-J., Hsu, Ch.-L., Hsueh, T. J., Shieh, T.-Y., *Sensors*, **2010**, *10*, 3057.

[14]Park, S., Jun, J., Kim, H. W., Lee, C., *J. Korean Phys. Soc.*, **2009,** *55*, 1591.

[15]Zhong, M. Y. Li, Tokizono, T., Zheng, M., Yamada, I., Delaunay, J.-J. , *J. Nanopart. Res.*, **2012,** *14*, 10 pp.

[16]Hayden, O., Greytak, A. B., Bell, D. C., *Adv. Mater.* **2005,** *17*, 701.

[17]Hu, Y., Kuemmeth, F., Lieber, Ch. M., Marcus. Ch. M., *Nat. Nanotechnol.*, **2012,** *7*, 47.

[18]Choi, H.-J., Johnston, J.C., He, R., Lee, S. K., Kim, F., Pauzauskie, P., Goldberger, J., Saykally, R. J., Yang, P. *J. Phys. Chem. B,* **2003,** *107*, 8721.

[19]Hochbaum, A. I. , Yang. P., *Chem. Rev.*, **2010**, 110, 527.

[20]Hollingsworth, J. A., Werner, J. H., Htoon, H., Piryatinski, A., Schaller, R., Ghosh, Y., Dennis, A. M., Keller, A. M., Mangum, B., Hannah, D. C., In: *Proc. Int. Conf. "Lasers and Electro-Optics (CLEO)"*. **2013,** San Jose.

[21]Jishiashvili, D., Chkhartishvili, L., Kiria, L., Shiolashvili, Z., Makhatadze, N., Jishiashvili, A., Gobronidze, V., *Nano Studies*, **2013,** *7*, 27.

[22]Dirtu, D., Odochian, L., Pui, A., Humelnicu, I., *Cent. Eur. J. Chem.*, **2006**, *4*, 666.

[23]Pakdehi, Sh. G., Salimi, M., Rasoolzadeh, M., *Res. Appl. Mech. Eng.*, **2014,** *3*, 21.

[24]Konnov, A. A., Ruyck, J. D., *Combust. flame*, **2001**, *124*, 106.

[25]Zheng, M., Cheng, R., Chen, X., Li, N., Li, L., Wang, X., Zhang, T. *Int. J. Hydrogen Energy*, **2005,** *30*, 1081.

[26]Jishiashvili, D., Kiria, L., Shiolashvili, Z., Makhatadze, N., Miminoshvili, E., Jishiashvili, A. *J. Nanosci.*, **2013,** *2013*, 10 pp.

[27]Xie, T., Jiang, Z., Wu, G., Fang, X., Li, G., Zhang, L., *J. Cryst. Growth*, **2005,** *283*, 286.

[28]Gao, Y. H., Bando, Y., Sato, T., *Appl. Phys. Lett.*, **2001,** *79*, 4565.

[29]Vallés, C., Núñez, J. D., Benito, A. M., Maser, W. K., *Carbon*, **2012,** *50*, 835.

[30]Gorbenko, V. I., Gorban, A. N., *Radiophysics (in Russian).* **2012,** *1*, 7.

[31]Gorbenko, V. I., Shvets, J. A., Gorban. A. N., In: *III–Nitride Based Semiconductor Electronics and Optical Devices and Thirty-Fourth State-of-the-Art Program on Compound Semiconductors (SOTAPOCS XXXIV).* In: *Proc. Int. Symp. 2001 – Technol. & Eng.* **2001**, Electrochem. Soc., 218.

[32]Akiyama, T., Nakamura, K., Ito, T., *Phys. Rev. B.*, **2006,** *73*, 235308, 6 pp.

[33]Dubrovskii, V. G., Sibirev, N. V., *Phys. Rev. B.*, **2008,** *77*, 035414, 8 pp.

[34]Li, J., Wang, D., la Pierre, R. R., *Advances in III–V Semiconductor Nanowires and Nanodevices. Bentham Sci. Publ.* **2011.**

[35]Moewe, M. J., Thesis (Elect. Eng. & Comp. Sci.). **2009,** Univ. CA Berkeley.

[36]Han, N., Wang, F., Yang, Z., Yip, S. P., Dong, G., Lin, H., Fang, M., Hung, T. F., Ho, J. C., *Nanoscale Res. Lett.*, **2014,** *9*, 6.

[37]Cao, G., Limmer. S. J., *Oxide Nanowires and Nanorods.* In: *Encyclopedia of Nanoscience and Nanotechnology*, *Am. Sci. Publ.*, **2004**

Received: 29.12.2014.
Accepted: 23.01.2015.